Low-temperature specific heat of antiferromagnetic $EuNi_5P_3$ and mixed-valent $EuNi_2P_2$ in magnetic fields to 7 T

R. A. Fisher
Materials Sciences Division, Lawrence Berkeley Laboratory and Department of Chemistry, University of California, Berkeley, California 94720

P. Radhakrishna
Materials Sciences Division, Lawrence Berkeley Laboratory and Department of Chemistry, University of California, Berkeley, California 94720
and Physics Department, Indian Institute of Science, Bangalore 12, India

N. E. Phillips, J. V. Badding,* and A. M. Stacy
Materials Sciences Division, Lawrence Berkeley Laboratory and Department of Chemistry, University of California, Berkeley, California 94720
(Received 31 July 1995)

The specific heats of $EuNi_5P_3$, an antiferromagnet, and $EuNi_2P_2$, a mixed-valence compound, have been measured between 0.4 and 30 K in magnetic fields of, respectively, 0, 0.5, 1, 1.5, 2.5, 5, and 7 T, and 0 and 7 T. In zero field the specific heat of $EuNi_5P_3$ shows a λ-like anomaly with a maximum at 8.3 K. With increasing field in the range 0–2.5 T, the maximum shifts to lower temperatures, as expected for an antiferromagnet. In higher fields the antiferromagnetic ordering is destroyed and the magnetic part of the specific heat approaches a Schottky anomaly that is consistent with expectations for the crystal-field/Zeeman levels. In low fields and for temperatures between 1.5 and 5 K the magnetic contribution to the specific heat is proportional to the temperature, indicating a high density of excited states with an energy dependence that is very unusual for an antiferromagnet. The entropy associated with the magnetic ordering is $\sim R$ ln8, confirming that only the Eu^{2+}—with $J=\frac{7}{2}$, $S=\frac{7}{2}$, $L=0$—orders below 30 K. In zero field approximately 20% of the entropy occurs above the Néel temperature, consistent with the usual amount of short-range order observed in antiferromagnets. The hyperfine magnetic field at the Eu nuclei in $EuNi_5P_3$ is 33.3 T, in good agreement with a value calculated from electron-nuclear double resonance measurements. For $EuNi_2P_2$ the specific heat is nearly field independent and shows no evidence of magnetic ordering or hyperfine fields. The coefficient of the electron contribution to the specific heat is ~ 100 mJ/mol K^2.

I. INTRODUCTION

The ternary phosphide compounds containing both rare-earth and transition metals are of particular interest because of the rich variety of crystallographic structures and the resulting complex interactions that lead to unusual magnetic orderings. In this paper we report measurements of the specific heat (C) of two members of this family of compounds— $EuNi_5P_3$, a recently synthesized[1,2] antiferromagnet with unusual magnetic properties, and $EuNi_2P_2$, a mixed-valence compound.

A. $EuNi_5P_3$

$EuNi_5P_3$ has an orthorhombic, centrosymmetric structure, $Cmcm$, corresponding to group No. 63 in the International Crystallographic Tables, and is isotypic with $LaCo_5P_3$ and $LaNi_5P_3$,[2] the only other rare-earth–transition-metal pnictides.[1,2] There are four formula units per unit cell and all of the Eu atoms occupy equivalent positions. Along the **a** axis the Eu-Eu distance is 3.62 Å, while for any other direction the separation is greater than 6 Å. Neutron powder diffraction shows that the magnetic unit cell is double that of the crystallographic unit cell.[1,3] The measurements did not distinguish between doubling along the **b** or **c** axis. However, a plausible magnetic structure, consistent with the neutron-diffraction and magnetization (M) measurements,[1,4] would be an antiferromagnetic arrangement of ferromagnetic chains of Eu^{2+} with the magnetic moments aligned parallel to the **a** axis and with a doubling of the unit cell along the **c** axis.

Above 100 K the magnetic susceptibility[1,4] (χ) of a single crystal of $EuNi_5P_3$ follows a Curie-Weiss law with $[g^2S(S+1)]^{1/2}\mu_B = 8.02\mu_B$, which is close to the free-ion value of $7.94\mu_B$ for Eu^{2+} ($4f^7, {}^8S_{7/2}$), while the saturation magnetic moment is $6.77\mu_B$, which is also close to the free-ion value $7\mu_B$.[5] Any contribution from the potentially magnetic Ni ions below 300 K is either very small or zero.

Below the Néel temperature (T_N), 8.3 K, the temperature (T) and magnetic field (H) dependence of M are unusual. For $H<0.5$ T, the T dependence of M is that of a typical antiferromagnet with magnetic ordering along the **a** axis. Along the **a** axis the magnetic behavior is dramatically different for $H>0.5$ T. As H is increased at constant T, M rises in a series of steps, with no obvious pattern to the step positions or their magnitude, until it reaches saturation for $H\sim 1$ T for $T=4.3$ K. For $H>0.5$ T the magnetization for this axis shows pronounced hysteresis in both H and T in the

antiferromagnetic region, and long times are necessary for equilibrium following changes in either T or H. Above T_N the steps vanish and M rises smoothly to saturation with increasing H, with short equilibration times and no hysteresis. Partial substitution of Ca^{2+} for Eu^{2+} reduces the equilibrium times and eliminates some, but not all, of the steps in the magnetization.[1] Along both the **b** and **c** axes, M varies smoothly with H at constant T and linearly at all T and low H, and rounds into saturation for $H>4T$. No hysteresis is observed along these two axes. The origin of the steps in M, when H is along the **a** axis, might be associated with multiple spin flops, which would indicate a complex magnetic structure.[1,4] In zero field, the electrical resistivity of $EuNi_5P_3$ is characteristic of a metal both in magnitude and temperature dependence.[1,4]

B. $EuNi_2P_2$

Marchard and Jeitschko synthesized $EuNi_2P_2$ in 1977 using the tin-flux method.[6] It crystallizes in the body-centered-tetragonal $ThCr_2Si_2$ structure, with space group D_{4h}.[6] Magnetic susceptibility and Mössbauer experiments[7] show that $EuNi_2P_2$ has no hyperfine field at the Eu nuclei and does not order magnetically for $T\geq 1.4$ K. Below ~ 40 K the susceptibility is temperature independent. Contributions to χ from the Ni ions are small or zero, as in $EuNi_5P_3$. The Mössbauer measurements show that $EuNi_2P_2$ is a mixed-valence compound, which maintains its mixed valency as $T\rightarrow 0$. It is the first Eu-based material to exhibit this behavior. While other Eu compounds have mixed valency at intermediate temperatures, the valence (v) approaches $+3$ as $T\rightarrow 0$.

A simple model[8] that has been applied successfully to intermediate-valence compounds is useful in interpreting the properties of $EuNi_2P_2$. In this model T is replaced by a temperature T^* defined as $T^*\equiv(T^2+T_f^2)^{1/2}$, and T_f is a characteristic temperature that measures the width of the sublevels—taken to be the same for all levels of both configurations. This width k_BT_f is due to the interconfigurational fluctuations of the system. In the model the ground states of the two multiplet configurations are separated by an energy ΔE. For $EuNi_2P_2$ it was assumed[7] that both T_f and ΔE were independent of temperature and that ΔE was the energy difference between the nonmagnetic ground state of Eu^{3+} ($4f^6,{}^7F_0$) and the ground state of Eu^{2+} ($4f^2,{}^8S_{7/2}$). The ratio of the partition functions for Eu^{2+} and Eu^{3+}—$Q_2(\Delta E,T^*)/Q_3(T^*)$—gives the ratio of 2^+ to 3^+ ions. The magnetic susceptibility of the system is given by $\chi(T)=[Q_2\chi_2(\Delta E,T^*)+Q_3\chi_3(T^*)]/(Q_2+Q_3)$, where $\chi_2(\Delta E,T^*)$ is the Curie susceptibility of the $4f^7$ ions and $\chi_3(T^*)$ is the Van Vleck susceptibility of the $4f^6$ ions. A fit to the susceptibility data yielded $T_f=80$ K and $\Delta E/k_B=160$ K, with excellent agreement between the measured and calculated values. The average valence of the system is given by $\langle v\rangle=(2Q_2+3Q_3)/(Q_2+Q_3)$, which varies from 2.5 for $T=0$ to 2.25 at 300 K.

II. SAMPLES AND MEASUREMENTS

The sample of $EuNi_5P_3$, 5.6226 g of powder, was prepared by slow heating of a stoichiometric mixture of the elements to 900 °C, with a small amount of I_2 (1 at. %) to catalyze the reaction, in an evacuated quartz tube for 1 week. The mixture was not allowed to melt. After rapid cooling and grinding, the heating cycle was repeated under the same conditions. Magnetic susceptibility measurements on the specific-heat sample gave values for both the Curie constant and saturation magnetization that were 8% lower than those obtained for a small single crystal (prepared later by pulling from a melt) and did not show evidence of other magnetic materials, suggesting the presence of approximately 8% of nonmagnetic impurities. An x-ray powder pattern showed a number of faint lines that were not identifiable. Details of the sample preparation and its characterization are given in Ref. 1. A sample of $EuNi_2P_2$, 1.0661 g of small crystals, was prepared by crystallization from a tin-flux solution of the elements.[6]

The polycrystalline samples were attached to a high-purity copper plate with GE7031 varnish, which was cured for 1 h at 100 °C. The plate was centered in a superconducting solenoid and connected by a high-purity silver rod to a calibrated germanium thermometer that was outside the solenoid and inside a superconducting shield of Nb that was held at ≤ 4.2 K. This arrangement shielded the thermometer from fringing fields of the solenoid and eliminated the necessity for its calibration in a field. A heater was attached to the silver rod near the sample.

Specific-heat measurements were made using a semiadiabatic heat-pulse method. This method utilizes two precision voltage supplies that can be rapidly switched (switching time ~ 1 ms) as alternate sources of heater power. The voltages necessary to produce $dT/dt\approx 0$ are determined in a separate experiment at the initial and final T's for each specific-heat point. For each point, one voltage supply is used to establish an initial drift with $dT/dt\approx 0$. To initiate the heat pulse, the second voltage supply is switched with the first for a preset period of time. At the end of this heating period the voltage supplies are again interchanged, but during the energy pulse the voltage of the first supply had been reset to the value needed to produce $dT/dt\approx 0$ for the afterdrift, which is also the foredrift for the next point. An extrapolation of the fore- and afterdrifts to the midpoint of the heating period establishes ΔT for the measurement. The energy associated with the measured ΔT is calculated by subtracting the average of the power necessary to establish the fore- and afterdrifts for the pulse from the power applied in the pulse itself. For these samples, the drifts after the heat pulse reached a steady state within less than 1 min. The precision of the total specific heat—sample plus addenda—is typically about $\pm 0.1\%$, while the accuracy is approximately $\pm 0.5\%$, as established by measurements of C for copper in fields to 7 T. For all measurements reported in this paper, the heat capacity of the addenda was less than one-half the total.

III. RESULTS, DATA, ANALYSIS, AND DISCUSSION

A. $EuNi_5P_3$

Figure 1 shows the specific-heat data for $EuNi_5P_3$ as C vs T. The solid curve represents the lattice specific heat (see below). For $H=0$ there is a λ-like anomaly with its maximum at 8.3 K. As H is increased to 0.5, 1, 1.5, and 2.5 T, the anomaly persists, but it becomes attenuated in magnitude, broadened, and shifted to lower temperatures. This behavior

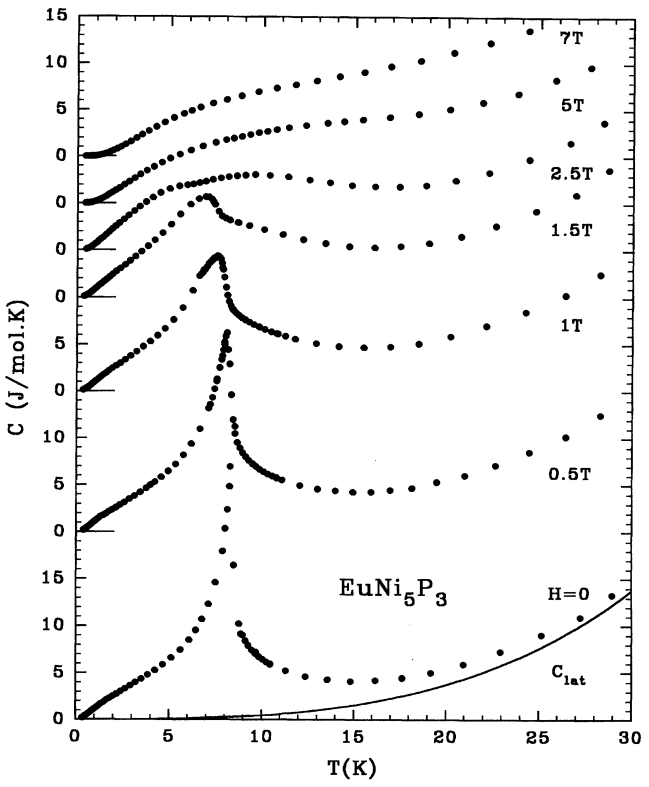

FIG. 1. Specific heat of the polycrystalline $EuNi_5P_3$ sample. The data for different magnetic fields are progressively displayed for clarity. The solid curve, $C_{\rm lat}$, represents the lattice contribution. (As shown here the data are not corrected for the presence of nonmagnetic impurities—see text.)

is typical of antiferromagnetic ordering. For $H=5$ and 7 T, C exhibits Schottky-like anomalies, which indicate that in these fields the antiferromagnetic ordering has been replaced by a paramagnetic state of the Eu^{2+} ions. The values of T_N, taken to be T at the maxima in C after subtraction of the lattice contribution, were derived by numerical differentiation with respect to T. For $H=2.5$ T, two maxima, located at ~ 5.8 and ~ 9.0 K, were obtained. The lower of these was taken as T_N, but that value is not as well defined as those for $H<2.5$ T because of the two broad and overlapping features in C.

For the purpose of data analysis, the contributions to the specific heat are assumed to be additive. They include the lattice ($C_{\rm lat}$) and the conduction electron ($C_{\rm el}$) contributions, both of which are assumed to be independent of H; a contribution arising from the Eu^{2+} ordering ($C_{\rm mag}$); and the hyperfine specific heat ($C_{\rm hyp}$) arising from the interaction of the nuclear magnetic moments of Eu with an effective magnetic field ($H_{\rm eff}$), the resultant of the applied field and the internal field of the ordered Eu^{2+} electronic moments. $C_{\rm lat}$ is represented by the usual harmonic lattice series in odd powers of T,

$$C_{\rm lat}=B_3T^3+B_5T^5+B_7T^7+\cdots, \tag{1}$$

and $C_{\rm el}$ by

$$C_{\rm el}=\gamma T. \tag{2}$$

There is no general expression for $C_{\rm mag}$, but in the high-temperature limit it can be represented by a series in T^{-n} ($n=2,3,4,\ldots$),

$$C_{\rm mag}(H)=\Sigma A_n(H)T^{-n}, \tag{3}$$

and for sufficiently large H/T by

$$C_{\rm mag}(H)=[b_1(H)/T^2]\exp[-b_2(H)/T]. \tag{4}$$

Equations (3) and (4) are, respectively, the high-T and low-T limiting forms of a Schottky function. In the temperature range of interest, $C_{\rm hyp}$ is adequately represented by the first term in the high-temperature limiting form of a Schottky function,

$$C_{\rm hyp}(H)=D(H)T^{-2}, \tag{5}$$

with

$$D(H)=(N_A/3k_B)\Sigma n_I[(I+1)\mu^2/I]H_{\rm eff}^2(H), \tag{6}$$

where N_A and k_B are the Avogadro number and Boltzmann constant, and the sum is over all isotopes with fractional abundance n_I, spin I, and magnetic moment μ.

The analysis of the specific heat into its components is complicated by the fact that $C_{\rm lat}$ makes a major contribution only at high T while $C_{\rm el}$ and $C_{\rm hyp}$ make major contributions only at low T. Nevertheless, it has been possible to obtain a consistent, plausible, and reasonably unique separation of the four components. The procedure was to analyze the data for $10\leq T\leq 30$ K *for all fields simultaneously*, using Eqs. (1), (2), and (3) to obtain provisional values for γ and the coefficients in the expansion for $C_{\rm lat}$. The provisional values for $C_{\rm lat}$, which is a relatively small contribution for $H=7$ T and $T<1$ K, were used to analyze the 7-T specific-heat data for $T\leq 1.1$ K to obtain $D(7\ {\rm T})$ and a more accurate value of γ. Finally, the analysis for the data in the $10\leq T\leq 30$ K range was repeated with γ fixed at the value obtained from the low-temperature fit to the 7-T data to obtain final values for the coefficients of $C_{\rm lat}$.

In the initial fit to the 10–30 K data, it was necessary to use two terms of Eq. (3) for $H\leq 2.5$ T and three terms for $H=5$ and 7 T. Surprisingly, only the T^3 and T^5 terms in Eq. (1) were necessary, and furthermore the coefficient of the T^5 term was relatively small. [The inclusion of higher-order terms of Eq. (1) did not significantly improve the fit.] This fit gave $\gamma=16.1$ mJ/mol K^2, $B_3=0.443$ mJ/mol K^4, and $B_5=7.47\times 10^{-5}$ mJ/mol K^6, with a rms deviation of 1.2%.

Figure 2 shows $(C\text{-}C_{\rm lat})/T$ vs T for the low-T 5- and 7-T data. (The figure was made using the final values of $C_{\rm lat}$, but these values are not significantly different from the provisional values derived in the first fit described above. Note that the curves in this figure are "guides to the eye": They do not represent fits to the data.) The contributions to $(C\text{-}C_{\rm lat})/T$ are γ; $D(H)/T^3$, the small upturn on the low-T side; and $C_{\rm mag}/T$, the upturn on the high-T side. For $H=7$ T, $C_{\rm mag}$ is small enough—i.e., H/T is high enough—that $C_{\rm mag}(7\ {\rm T})$ is adequately represented by Eq. (4). The 7-T data for $T<1.2$ K are well represented by Eqs. (2), (4), and (5), and fits with these relations gave $\gamma=17.5$ mJ/mol K^2 and $D(7\ {\rm T})=2.19$ mJ K/mol. The quality of the fit is illustrated

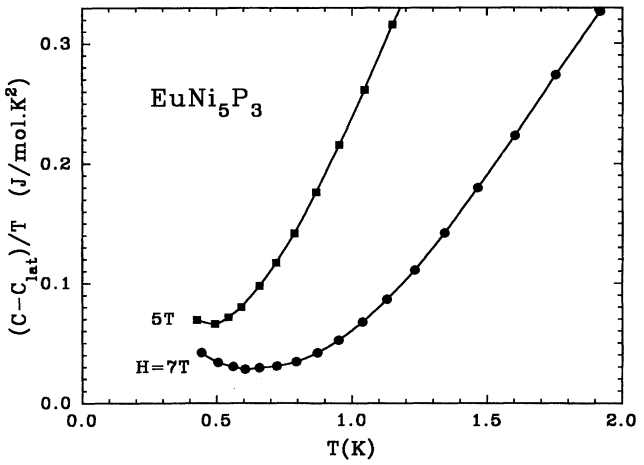

FIG. 2. Low-T, 5- and 7-T data for the $EuNi_5P_3$ sample displayed as $(C\text{-}C_{lat})/T$ vs T. The solid curves are "guides to the eye" and do not represent fits. (As shown here the data are not corrected for the presence of nonmagnetic impurities—see text.)

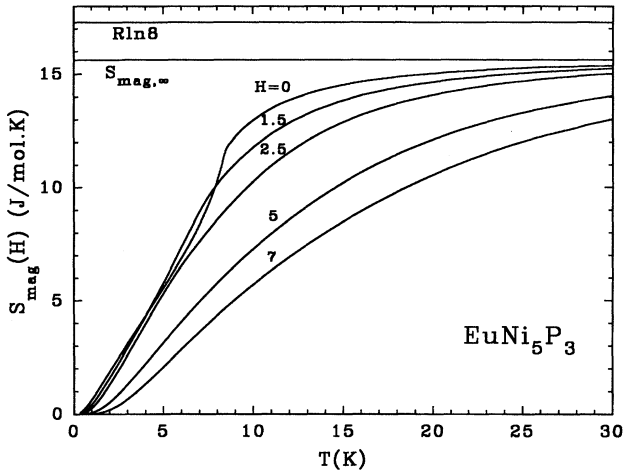

FIG. 4. $S_{mag}(H)$ vs T for $EuNi_3P_3$. Data for $H=0.5$ and 1 T, which are very similar to those for $H=0$, are omitted for clarity. The line at $R\ln 8$ indicates the expected value of $S_{mag,\infty}$; the one labeled $S_{mag,\infty}$ represents approximately the values obtained by extrapolation of the specific-heat data, uncorrected for nonmagnetic impurities, to $T=\infty$.

for $T \leq 1$ K in Fig. 3 as a plot of $(C\text{-}C_{lat}\text{-}C_{mag})T^2$ vs T^3 in which $D(7\text{ T})$ is given by the intercept and γ by the slope. [For the 5-T data, Eq. (4) does not give an adequate representation of C_{mag} (H is too low and T is not low enough) and this type of analysis is not possible.]

The value of γ derived from the low-T data is about 9% higher than that derived in the first fit to the 10–30 K data. However, constraining γ to the higher value in the 10–30 K fit has only a small effect on the derived value of C_{lat} because C_{el} makes only a small contribution in that region. Repeating the 10–30 K fit with γ fixed at 17.5 mJ/mol K^2 gave $B_3=0.440$ mJ/mol K^4 (a reduction of 0.7% from the provisional value obtained in the first fit with γ taken as an adjustable parameter) and $B_5=7.71\times10^{-5}$ mJ/mol K^6 (a 3% increase, but in a term that makes a smaller contribution). At

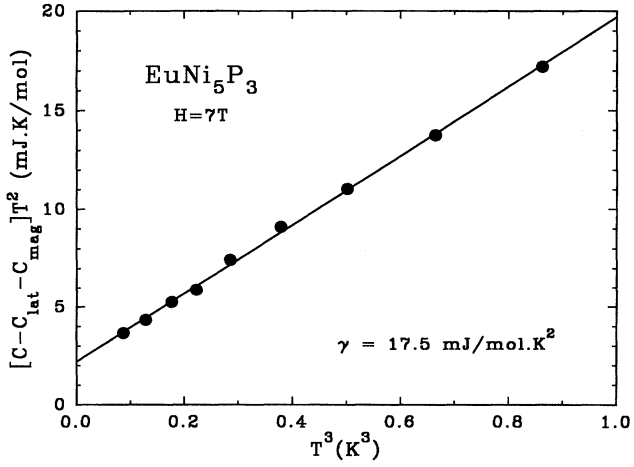

FIG. 3. $(C\text{-}C_{lat}\text{-}C_{mag})T^2=D+\gamma T^3$ vs T^3 for the $EuNi_5P_3$ sample and $H=7$ T. The solid line represents a least-squares fit that gave the values of $D(7\text{ T})$ and γ. (As shown here the data are not corrected for the presence of nonmagnetic impurities—see text.)

30 K the changes in B_3 and B_5 largely cancel, leaving C_{lat} essentially unchanged. To two significant figures the rms deviation was 1.2%, the same as in the first fit. The relatively small differences in the value of parameters obtained in the different steps of the analysis and the consistency of the extrapolated values of the magnetic entropy (see below) attest to the consistency of the data with the fitting expressions.

Figure 4 shows the magnetic entropy (S_{mag}) obtained by numerical integration of C_{mag}/T with respect to T. Appropriate extrapolations of C_{mag} to $T=0$ were made to obtain the small (0.0–0.3 % of R ln8) entropy contributions for $T \leq 0.4$ K. The curves for $H=0.5$ and 1 T are so close to that for $H=0$ that they have been omitted for the sake of clarity. The figure suggests, particularly obviously for the low-H data, that S_{mag} does not approach the value $R\ln 8$ expected for 1 mol of Eu^{2+} in the high-T limit. In fact, extrapolation of C_{mag} to $T=\infty$ using the coefficients in Eq. (3) obtained in the 10–30 K fits gives values of S_{mag} in the limit $T=\infty$ ($S_{mag,\infty}$) $S_{mag,\infty}/R$ ln8=0.90 for 0, 0.5, 1, and 1.5 T, 0.91 for 2.5 T, and 0.93 for 5 and 7 T. These extrapolations are most reliable for the low fields, for which their contributions to $S_{mag,\infty}$ are small (1–4 % for $H=0$–2.5 T) suggesting $0.90R\ln 8$, represented by the horizontal line labeled S_{mag} in Fig. 4, as the best value for that quantity. However, the magnetization data described in Sec. II show that C_{mag} and S_{mag} should be corrected for the presence of approximately 8% of nonmagnetic impurities. Thus, to within an uncertainty of 1–2 %, $S_{mag,\infty}$ can be taken as agreeing with the value expected for Eu^{2+}, R ln8. The specific-heat contributions of most interest, C_{hyp} and C_{mag}, have been corrected, therefore, by the factor 1/0.90, which corresponds to the assumption that $S_{mag,\infty}=R$ ln8. This correction has been incorporated into the data plotted in Figs. 5–7; its application to the parameters derived from C_{hyp} gives 2.43 mJ K/mol for $D(7\text{ T})$. There is no comparably straightforward basis for correcting C_{lat} and C_{el} for the presence of the impurities.

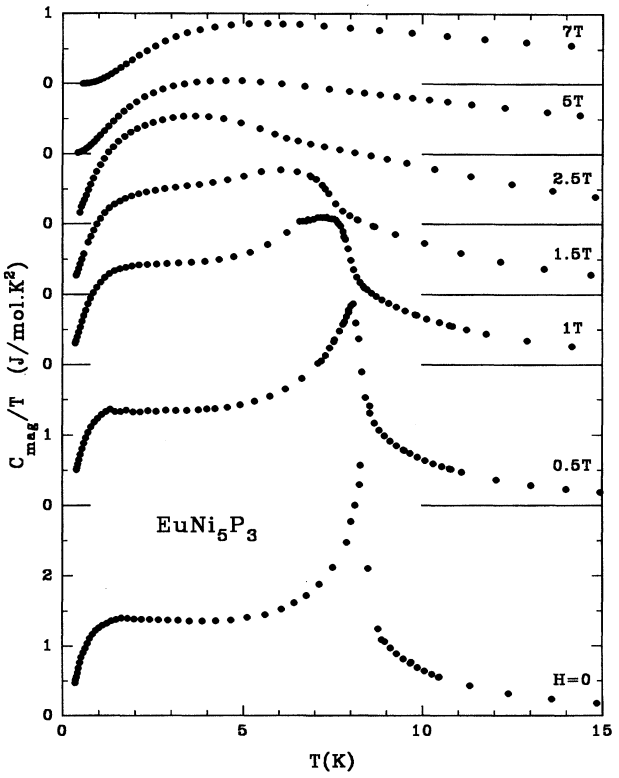

FIG. 5. C_{mag}/T vs T for $EuNi_5P_3$.

However, the correction to C_{lat}, which is of relatively little interest, is probably small. The correction to C_{el}, which would depend on whether the impurities are metallic or not, could be substantial: In the extreme, but improbable, case that 5% of $EuNi_2P_2$ was present (an amount that might not have been detected in the x-ray analysis) its very high value

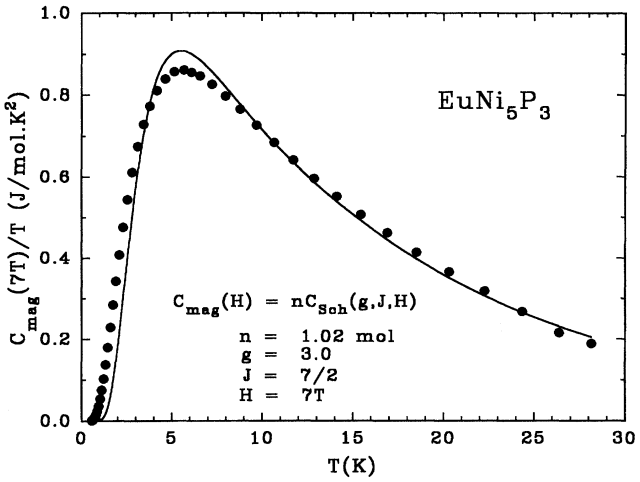

FIG. 7. Approximate representation of $C_{\mathrm{mag}}(7\ \mathrm{T})$ for $EuNi_5P_3$ by a Schottky function.

of γ (see below) would have led to a contribution of 5 mJ/mol K^2 to the measured value 17.5 mJ/mol K^2.

The specific heat associated with the ordering of the Eu^{2+} ions is shown as C_{mag}/T for $T \leq 15$ K in Fig. 5. For $H=0$ there is a sharp λ-like feature at T_N that rules out the possibility of one-dimensional ordering for which a more Schottky-like specific-heat anomaly would be expected. At $T>T_N$ the long high-T "tail" in C_{mag}, which is associated with short-range order and makes a contribution of ~20% to $C_{\mathrm{mag},\infty}$, is typical of antiferromagnets. At $T<T_N$ and approximately in the temperature range 1.5–5 K, there is a feature that is unusual for antiferromagnets, a "plateau" in C_{mag}/T with a magnitude of 1.39 J/mol K^2, which occurs between a rapid decrease in C_{mag}/T at lower temperatures and the peak at T_N. This plateau indicates a spectrum of magnetic excitations with an approximately energy-independent density of states in the corresponding energy

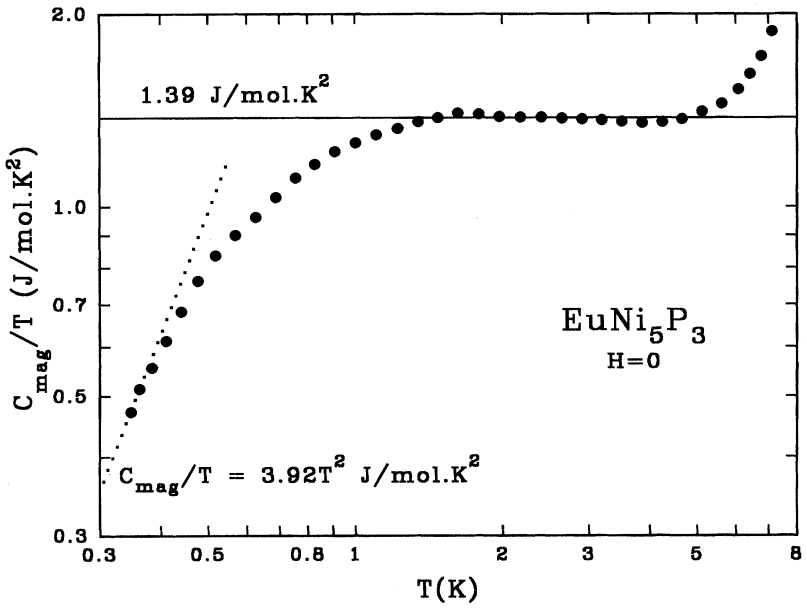

FIG. 6. Log-log plot of C_{mag}/T vs T for $EuNi_5P_3$ illustrating the region of approximately constant C_{mag}/T and the apparent approach to constant C_{mag}/T^3 in the low-T limit.

range. This constant and high density of states may be related to the unusual magnetic properties found for H parallel to the **a** axis. At the lowest temperatures at which C was measured, $C_{\rm mag}$ approaches the T^3 dependence expected for spin waves in a three-dimensional antiferromagnet with no energy gap in the excitation spectrum, $C_{\rm mag}/T^3 = 3.92$ J/mol K^4 (see Fig. 6).

The critical magnetic field, the field necessary to suppress antiferromagnetic ordering for a given temperature, is generally smaller in the direction parallel to the alignment axis than in a perpendicular direction. The magnetization measurements on single crystals of $EuNi_5P_3$ (Refs. 1 and 4) have established that the easy axis is along **a** with a critical field at 4 K of ~ 1 T, while in the perpendicular directions, along either the **b** or **c** axis, the critical field at 4 K is ~ 4 T. (The critical field for the **c** axis is a few percent greater than that for the **b** axis.) For a randomly oriented polycrystalline sample and $1 \leq H \leq 4$ T, the sample will consist of both paramagnetic and canted regions, which depend on the relative orientation of the field and crystallites. This partial suppression of antiferromagnetism for a polycrystalline sample provides a basis for understanding the evolution of the T dependence of $C_{\rm mag}$ with increasing H. For $H \leq 1$ T all of the sample has antiferromagnetic or canted order below T_N, while for $H \geq 1$ T the antiferromagnetic order is destroyed in some of the material. The occurrence of both a shoulder and a maximum in C for $H = 2.5$ T (see Fig. 1) can also be understood on this basis. The shoulder is due to canted order in some of the sample, while the maximum at higher temperature has its origin in a Schottky-like anomaly associated with material that is paramagnetic. For $H = 5$ and 7 T, all canted order has disappeared, and the anomalies have assumed a Schottky-like appearance. This is illustrated more clearly for the 7-T data in Fig. 7, where they are compared with a Schottky function. It is not possible to calculate the specific heat for a polycrystalline sample because of the initial splitting of the $4f^7$, $^8S_{7/2}$ ground-state manifold for Eu^{2+} that results from the admixture of higher-lying states, the nonlinear divergence of the energy levels in a magnetic field, the random orientations of the crystallites, and the interactions between ions. (Admixtures of higher-lying states and crystal-field splitting of this manifold are expected to result in a ground-state doublet and an excited quadruplet lying below a second doublet, with the separations between the groups of levels small in zero field.[5]) The specific heat can be represented approximately, however, by a Schottky function, $nC_{\rm Sch}(g,J,H)$, with $J = 7/2$, $H = 7$ T, and g and the number of moles of Eu^{2+}, n, allowed to vary. Although g is known to be ~ 2 for Eu^{2+},[5] an approximate accounting can be made for the greater-than-Zeeman spacing of the energy-level manifold in 7 T—due to the zero field splitting—by allowing it to be a variable of the fit. The solid curve in Fig. 7 represents the Schottky fit to the data with the fit parameters given in the figure. In view of its approximate nature, the fit is reasonably good; furthermore, the value of n, 1.02 mol Eu^{2+}, is consistent with the slightly higher value of $S_{\rm mag,\infty}$ found for the 7-T data than the value used to normalize $C_{\rm mag}$.

The variation of T_N with H, deduced from the maxima in C for $H = 0$, 0.5, 1, and 1.5 T, and the shoulder in C for 2.5 T, is shown in Fig. 8. $T_N(H)$ shows the decrease in temperature with increasing H that is typical of antiferromagnetic ordering. The points are fitted by the expression,

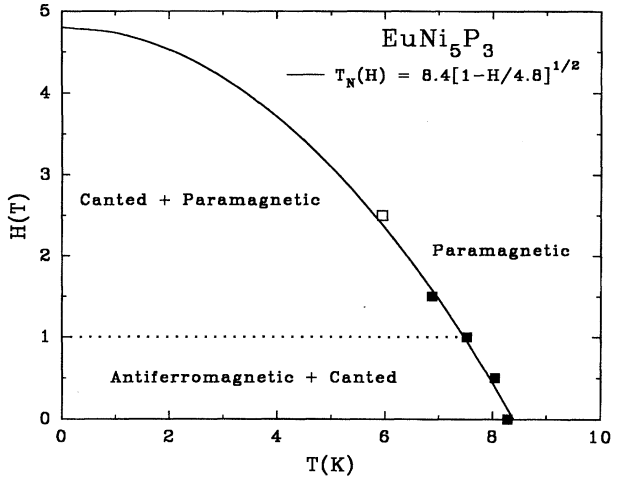

FIG. 8. "Phase diagram" for the $EuNi_5P_3$ sample.

$$T_N(H) = T_N(0)[1 - H/4.8]^{1/2}, \tag{7}$$

shown as a solid curve, which extrapolates to 4.8 T at $T = 0$. For the randomly oriented crystallites this curve defines an upper limit to the magnetic field in which canted order exists. In the region labeled canted + paramagnetic, some crystallites are in a canted antiferromagnetic state and some are paramagnetic. In the region of the diagram below the horizontal dashed line at 1 T, no paramagnetic phase is present. Because the sample is polycrystalline, Fig. 8 is not a true phase diagram. However, it is probably not very different from the phase diagram for H applied parallel to the **c** axis of a single crystal. It should be noted that the extrapolated value of H at $T = 0$, 4.8 T, is close to the value of the field needed to saturate M at 4 K when H is applied along the **c** axis.[1,4]

The coefficient of the 7-T hyperfine term, evaluated from the data as shown in Fig. 3 and corrected for the presence of nonmagnetic impurities, is $D(7\ \text{T}) = 2.43$ mJ K/mol. Eu is the only element in $EuNi_5P_3$ with nuclear moments[9]—^{151}Eu (% abundance=47.77, $I = 5/2$, $\mu = 3.42\mu_N$) and ^{153}Eu (% abundance=52.23, $I = 5/2$, $\mu = 1.51\mu_N$)—and Eq. (6) gives $H_{\rm eff}$ (7 T)=26.3 T for the effective field at the Eu nuclei in an applied field of 7 T. Theory[5] predicts that the applied and internal hyperfine fields are antiparallel, to give 33.3 T for $H_{\rm eff}(0)$, the internal field. Taking into account the accuracy with which $H_{\rm eff}(7\ \text{T})$ is determined (as the square root of the intercept in Fig. 3) this is entirely satisfactory agreement with the value 34.5 T calculated by Bleaney[10] from electron-nuclear double resonance measurements by Baker and Williams on Eu^{2+} diluted in CaF_2.[11] In the case of Eu metal, Lounasmaa[12] derived $H_{\rm eff}(0) = 26.0 \pm 0.4$ T from specific-heat measurements in zero field, and Barrett and Shirley[13] deduced $H_{\rm eff}(0) = 26.4 \pm 0.8$ T from Mössbauer measurements. To explain the low value, Lounasmaa[12] conjectured that in the metal Eu might be mixed valent.

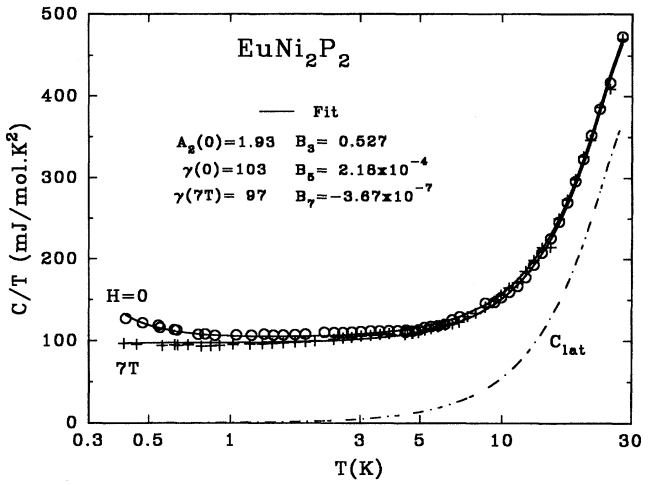

FIG. 9. Specific heat of polycrystalline $EuNi_2P_2$. The solid curves represent least-squares fits and the dot-dashed curve the lattice specific heat—see text for discussion.

B. $EuNi_2P_2$

The specific heats of $EuNi_2P_2$ in zero field and 7 T are shown in Fig. 9. Except for the upturn in $C(0)$ at low temperatures, no magnetic ordering is evident, and there is only a weak H dependence. The upturn is probably the "high-temperature tail" of a specific-heat anomaly associated with a small amount of magnetic impurity that orders primarily at still lower temperatures. However, the absence of a Schottky anomaly in $C(7\ \mathrm{T})$—such an anomaly is not apparent in the data as plotted in Fig. 9, and fits to the 7-T data are not improved by the inclusion of a Schottky function in the fitting expression—puts an upper limit of $\sim 10^{-3}$ mol/mol $EuNi_2P_2$ to the concentration of the impurity. There is also no evidence of a hyperfine term in the 7-T data. (Inclusion of a T^{-2} term for $H=7$ T in the fitting expressions does not improve the fit; the contribution calculated for the direct coupling of the Eu nuclei with the applied field is less than 2% for the lowest-temperature point.)

The solid curves in Fig. 9 represent the result of a fit to the $H=0$ and 7 T data with Eqs. (1), and (2), but the γ allowed to vary with H and, for $H=0$ only, the first term of Eq. (3). The rms deviation was 2.3%. Values of the parameters in C_{el} and C_{lat} derived from the fit are $\gamma(0)$ and $(7\ \mathrm{T})=103$ and 97 mJ/mol K^2, respectively; $B_3=0.527$ mJ/mol K^4, $B_5=2.18\times10^{-4}$ mJ/mol K^6, and $B_7=-3.67\times10^{-7}$ mJ/mol K^8. Inclusion of terms beyond the T^7 term in C_{lat} did not improve the fit.

The weak H dependence of C is consistent with the temperature-independent magnetic susceptibility below 40 K.[7] Also, the large value of γ, ~ 100 mJ/mol K^2, is typical of mixed-valence compounds. Since the ground state of the system is nonmagnetic Eu^{3+}, the internal hyperfine field is expected to be zero, as observed.

ACKNOWLEDGMENTS

This work was supported by the Director, Office of Basic Energy Sciences, Materials Sciences Division of the U.S. Department of Energy under Contract No. DE-AC03-76SF00098. P.R.'s participation was made possible by a visit to the University of California at Berkeley supported by the National Science Foundation Division of International Programs through Grant No. INT-9318199.

*Current address: Chemistry Department, The Pennsylvania State University, University Park, PA 16802.

[1] J. V. Badding, Ph.D. dissertation, Department of Chemistry, University of California, Berkeley, CA, 1989.

[2] J. V. Badding and A. M. Stacy, J. Solid State Chem. **67**, 354 (1987).

[3] Powder neutron-diffraction measurements were made by J.V.B. at Brookhaven National Laboratory in collaboration with D. E. Cox.

[4] J. V. Badding and J. M. Stacy, Phys. Rev. B **35**, 8880 (1987).

[5] A. Abragam and B. Bleaney, *Electron Paramagnetic Resonance of Transition Ions* (Clarendon, Oxford, 1970).

[6] R. Marchard and W. Jeitschko, J. Solid State Chem. **24**, 351 (1978).

[7] R. Nagarajan, G. K. Shenoy, L. C. Gupta, and E. V. Sampathkumaran, Phys. Rev. B **32**, 2846 (1985).

[8] E. R. Bäuminger, I. Felner, D. Froindlich, D. Levron, I. Nowik, S. Ofer, and R. Yanovsky, J. Phys. (Paris) Colloq. **35**, C6-62 (1974); B. C. Sales and D. Wohlleben, Phys. Rev. Lett. **35**, 1240 (1975); W. Franz, F. Steglich, W. Zell, D. Wohlleben, and F. Pobell, *ibid.* **45**, 64 (1980).

[9] I. Lindgren, Nucl. Phys. **32**, 151 (1962); B. R. Judd and I. Lindgren, Phys. Rev. **122**, 1802 (1961).

[10] B. Bleaney, J. Phys. Soc. Jpn. **17**, Suppl. B-I, 435 (1962); J. Appl. Phys. **34**, 1024 (1963).

[11] J. M. Baker and F. I. B. Williams, Proc. R. Soc. London A **267**, 283 (1962).

[12] O. Lounasmaa, Phys. Rev. **133**, 502 (1964).

[13] P. H. Barrett and D. A. Shirley, Phys. Rev. **131**, 123 (1963).